Int. J. Plant Sci. 169(8):998–1012. 2008.
This article is in the public domain, and no copyright is claimed.
1058-5893/2008/16908-0003$15.00 DOI: 10.1086/590442

THE VESTIGIAL ROOT OF DODDER (*CUSCUTA PENTAGONA*) SEEDLINGS

Timothy D. Sherman,*,† Andrew J. Bowling,† T. Wayne Barger,[1],† and Kevin C. Vaughn[2],†

*Department of Biological Science, University of South Alabama, Mobile, Alabama 36688, U.S.A.; and †USDA-ARS, Southern Weed Science Research Unit, Stoneville, Mississippi 38776, U.S.A.

Seedlings of dodder are unique among dicotyledonous plants in that they emerge as a leafless, cotyledonless shoot with only a small swollen rootlike structure at the base of the tissue. Although growth of the shoot end of the dodder seedling is dramatic, no change in "root" length occurs, and the root tip is withered and senescent within 7 d of germination. Unlike most roots, the dodder root has neither recognizable root cap nor apical meristem. A strand of vascular tissue extends all the way to the root apex and is already differentiated into vascular elements on germination. Cortical cells swell dramatically and contain large vacuoles with a small rim of cytoplasm. Nuclei in these cortical cells are extensively lobed and are much larger than nuclei in shoot tips, indicating endopolyploidy. Microtubules are detected, although they are much less abundant than in shoot tissue of dodder or roots of other dicots, especially in roots older than 1 d postgermination. Similarly, α-tubulin protein, as detected by immunoblots, appear as faint bands in root extracts; both are easily detectable in extracts of shoot tissue. Cell walls of 1–2-d-old roots are normal in morphology and contain well-defined cellulose microfibrils and well-developed middle lamellae. In contrast, later stages of development reveal cell-wall-loosening complexes and the degradation of wall structure and loss of polysaccharides, especially those of pectin side chains, which also are lost in other senescent tissues. By 5–7 d postgermination, all of the cortical cells have degenerated, leaving the vascular strand as the last remnant of intact tissue in these roots. From these data, we conclude that the swollen appearance of the dodder root is due to the low level of microtubules, so that neither mitotic divisions nor cell elongation can occur, and the loosening/senescence of the cell wall allows for expansion, resulting in a swollen root phenotype. It is speculated that the degeneration of the root end of the dodder may allow a flow of carbon from this organ to sustain the continued growth of the shoot. Although the tuberous end is clearly differentiated from the shoot tissue, it probably should be considered a highly modified basal portion of stem tissue used as a food reserve and basal support rather than a root.

Keywords: *Cuscuta*, dodder, microtubules, cell wall, parasitic weeds.

Introduction

Dodders (*Cuscuta* spp.) are the most widespread agronomically and economically important group of parasitic weeds (Kujit 1969). One of the reasons for their success is their ability to rapidly invade a wide range of species soon after seed germination (Vaughn 2003, 2006). Seedlings of dodder are streamlined for the attack of the host. They germinate as leafless, cotyledonless, almost chlorophyll-less seedlings (Kujit 1969; Dawson et al. 1994; Sherman et al. 1999). In fact, it has been argued, based on their unusual embryology, that the dodder seed does not contain an embryo but rather a dormant seedling (Rao and Rama Rao 1990). At the base of the seedling is a bulbous, swollen rootlike structure (Lyshede 1986). From this, the shoot grows rapidly and entwines the host, establishing a parasitic union in as little as a week after germination. During this period, however, the root tissue does not appear to grow and actually becomes senescent.

Most of the structural studies of dodders have centered on the parasitic habit of the mature plant, especially on the haustoria, which is the parasitic tissue machinery (Heide-Jorgenson 1987; Lee and Lee 1989; Dawson et al. 1994; Vaughn 2003, 2006; Lee 2007*a*). There is much in the dodder seedling, especially the root tissue, that appears to be unusual and deserves more attention structurally (Lyshede 1985, 1986, 1989; Lee 2007*b*). The terminal rootlike structure is of special interest. For example, LM studies have cast doubt on whether the dodder plant actually has a root at all (Haccius and Troll 1961; Truscott 1966). Several investigators have noted that the dodder rootlike structure lacks a root cap or apical meristem (Truscott 1966; Lyshede 1986). Although the dodder root has hairs, they are at the root tip rather than in the zone of differentiation and elongation as in other dicot roots. Dodder root tissue senesces rapidly, and complete disintegration of the root often occurs before parasitism takes place, indicating that the dodder root is not critical to water or nutrient uptake (Kujit 1969; Malik and Singh 1979). Because of the ephemeral nature of the root and its abnormal, swollen morphology, some morphologists have questioned whether the dodder root should be designated as a true root (Truscott 1966). In fact, Lyshede (1986) used the more apt term "tuberous radicular end" to describe this structure rather than "root."

In this study, we utilize a number of microscopic and biochemical methods in order to examine the dodder root and to readdress the question of whether the dodder root is truly a

[1] Current address: Department of Conservation, State Lands Division, 64 North Union Street, Montgomery, Alabama 36130, U.S.A.

[2] Author for correspondence; e-mail: kevin.vaughn@ars.usda.gov.

Manuscript received October 2007; revised manuscript received December 2007.

root or really some other specialized tissue and to determine the cause(s) for its swollen nature and rapid decline. For simplicity, we will use the term "root" for this basal rootlike structure of the dodder seedling throughout this article with the proviso that this structure may not have all the characteristics of a typical dicotyledon seedling root.

Material and Methods

Plants and Growth Studies

To break dormancy, seeds of *Cuscuta pentagona* (F and J Seed Service, Urbana, IL) were treated with concentrated sulfuric acid for 1 h at room temperature. They were rinsed in a concentrated solution of sodium bicarbonate and washed briefly in running distilled water. The seeds were then allowed to dry briefly before plating in tall glass petri dishes on 1.5% (w/v) nutrient media agar (Sommerville and Ogren 1982) supplemented with 0.01% (w/v) ampicillin to suppress bacterial growth. The culture dishes were held in a growth chamber with continuous irradiance of 125 μmol m^{-2} s^{-1} PAR and maintained at room temperature (~22°C). Shoot and root lengths were measured daily as an indicator of plant growth. Seedlings for microscopic evaluations were carefully monitored for time of germination so that variations in seed germination would not obscure the developmental studies. Some seedlings were also germinated in petri dishes on Whatman no. 1 filter paper moistened with water. These showed the same developmental patterns as those germinated on media. Onion seed (cv. "Red Hamburger") was germinated on moistened Whatman no. 1 filter paper in 9-cm petri dishes, and seedlings were grown in the dark for 3 d before harvesting.

Microscopy

Whole roots or root tips, cut open to enhance fixation and embedding, were fixed in 6% (v/v) glutaraldehyde in 0.05 M PIPES buffer (pH 7.4) for 2 h at room temperature. The samples were washed in two changes of 0.1 M cacodylate buffer (pH 7.2) before postfixation for 2 h in 2% osmium tetroxide in 0.1 M cacodylate buffer. After two water rinses, the samples were stained en bloc with 2% (w/v) uranyl acetate for 18 h at 4°C. Samples were washed extensively in water and dehydrated in an acetone series and transferred to propylene oxide. A 1 : 1 (v/v) mixture of Spurr's low-viscosity resin and Polybed 812 (Polysciences, Warrington, PA) was added in increasing increments to 75% plastic, with the remaining 25% of propylene oxide allowed to evaporate through small holes punched in aluminum foil covers over the sample vials. After this slow last infiltration step, fresh resin was added to the vials, and the samples were rocked on a gyratory shaker overnight to enhance plastic infiltration. The root tissues were embedded in flat embedding molds and mounted on acrylic stubs so that longitudinal sections through the root and shoot meristems could be obtained. Light sections (0.35–0.55 μm) were cut with a Delaware Diamond Histo Knife, and thin sections (gray-silver reflectance) were cut with a Delaware Diamond Knife on a Reichert Ultracut 2 ultramicrotome. Samples were observed with an LM after staining with 1% (w/v) toluidine blue in 1% (v/v) sodium borate or with a Zeiss EM10CR electron microscope operating at 60 kV after sequential uranyl acetate and lead citrate staining. Some fresh roots were stained with phloroglucinol or the Maule stain as indicators of lignin.

For SEM, the samples were fixed in 6% (v/v) glutaraldehyde in 0.1 M PIPES buffer (pH 7.4) for at least 2 h at 4°C. The samples were then washed, dehydrated, critical-point dried, and sputter-coated as previously described (Vaughn 2002*a*). Specimens were examined with a JEOL 840 SEM operating at 15 kV.

For immunogold-silver labeling at the LM level, samples were prepared according to Meloche et al. (2007). Essentially, samples were fixed in 3% (v/v) glutaraldehyde in PIPES buffer, dehydrated in an ethanol series, and embedded in LR White resin. Sections were probed with a battery of monoclonal antibodies that recognize specific polysaccharide moieties, decorated with immunogold antimouse or antirat IgG, and intensified with silver. Sections were imaged by LM using an Olympus Qcolor3 digital camera.

For immunogold TEM, sections of pale gold-silver reflectance were mounted on uncoated 300-mesh gold grids. The samples were processed as described previously (Vaughn 2002*a*) using antibodies described in several previous reports (Vaughn et al. 1996; Sabba et al. 1999; Vaughn 2002*a*; Bowling and Vaughn 2008). The density of immunogold labeling was quantified on a square-micron-of-cell-wall basis. Data from seven micrographs, each from three different localization experiments, were used in the analysis. Because of the wide tissue variance, only parenchyma cells near the vascular tissue were used in the comparisons.

Immunoblotting

The protocols used for electrophoresis and subsequent immunoblotting of dodder are described in detail in Sherman et al. (1999). Samples from both roots and shoots were used in the analysis. Equal protein loads were made for comparison. Acrylamide gels (7.5% w/v) were run in a Bio-Rad electrophoresis unit at 4°C. Gels were either stained with Coomassie blue or were electrophoretically transferred to nitrocellulose and probed with rat or mouse monoclonal antibodies and detected with alkaline phosphatase–labeled secondary antibodies. Monoclonal antibodies specific for actin and tubulins (Amersham, Arlington Heights, IL) were utilized at dilutions of 1 : 500–1 : 2000. As a comparison, extracts from roots from 3-d-old seedlings of onion were prepared in the same manner and run beside the dodder root and shoot extracts.

DNA Laddering Analysis

Nucleic acids were isolated using a modification of the method of Lodhi et al. (1994). Root or shoot tissue was homogenized in liquid nitrogen with a small metal blender cup and then further homogenized with a mortar and pestle under liquid nitrogen. Tissue was then combined with CTAB extraction buffer (100 mM Tris, 20 mM EDTA, 1.4 M NaCl, 2% (w/v) hexadecyltrimethylammonium bromide [CTAB], 0.2% [v/v] β-mercaptoethanol) that had been preheated to 60°C. The mixture was incubated for 30 min at 60°C with occasional mixing. Samples were then cooled to room temperature and extracted with one-half vol of chloroform : isoamyl alcohol. Nucleic acids were recovered from the aqueous phase by

precipitation after the addition of 0.5 vols of 5 M NaCl and 2 vols of 95% ethanol. Precipitated nucleic acids were centrifuged for 10 min at 1600 *g*. The resulting pellet was washed with cold 76% ethanol to remove residual CTAB. The pellet was then air dried, resuspended in TE (pH 8.0), and treated with DNAse-free 100 μg mL^{-1} RNAse A and 10 unit mL^{-1} RNAse T1 for 1 h at 37°C. DNA was quantified via fluorescence measurement using Hoechst 33258 (Cesarone et al. 1979). DNA was then examined for laddering by electrophoresis using a 0.8% (w/v) agarose gel in 0.5× TBE (Sambrook et al. 1989).

Results

Visual and General Growth Characteristics of Roots vs. Shoots

The dodder seedling emerges from the seed as early as 1 d after plating in our system. A small tuberous structure (herein described as the dodder "root"), ~2 mm in length, emerges from the seed coat (fig. 1*a*). The shoot tissue emerges subsequently and is relatively elongated and coiled. Even at this early time, the shoot area is distinctly yellow/orange with a slight green tinge near the tip. The root is paler than the shoot area, being virtually white and distinctly swollen by 2–3 d after germination (fig. 1*a*). The most extreme areas of swelling are just in back of the tip. After 7 d of plating on the agar, the shoot has grown considerably, from an average of 9.78 mm on day 3 to 93.6 mm on day 7, yet the root has not elongated at all. In fact, the average root has decreased in length from 3.62 mm after 3 d of growth to 1.98 mm at day 7. By the tenth day, the tuberous end of the seedling is completely collapsed and senescent, with tissue collapse extending into the basal areas of the shoot as well.

The dodder root tissue also does not display the normal geotropic responses of typical roots. In the controlled experiment conditions of the agar medium, the root remains on the surface. Similarly, under growth chamber conditions, when scarified dodder seeds are placed on potting mix, the roots neither penetrate the soil nor display any other positive or negative geotropic response (K. C. Vaughn, personal observations).

Survey of LM Changes in Root Tissue

To obtain a whole-tissue view of the changes that occur in the dodder root, three whole roots from each day (from day 1 through day 7 after germination) were serially sectioned longitudinally at 0.55-μm increments and examined by LM. Other roots were examined, but only through half the root until the vascular tissues (presumed to be halfway through the root) were detected. Another group was sampled and examined by whole-mount SEM (fig. 2). Although there were small differences in roots sampled from different dates, the results showed the same trends between six sets of experiments that occurred over several years. The most consistent samples were found in the 1-d-old seedlings. Thereafter, more variability was noted, especially in the 5–7-d-old samples.

Longitudinal sections through the roots of 1-d-old dodder seedlings reveal a distinctly different organization of tissue compared to the roots of typical dicot seedlings (fig. 3). Unlike other dicot seedling roots, dodder roots have no meristem or root cap. The vascular tissue extends to the very tip of the

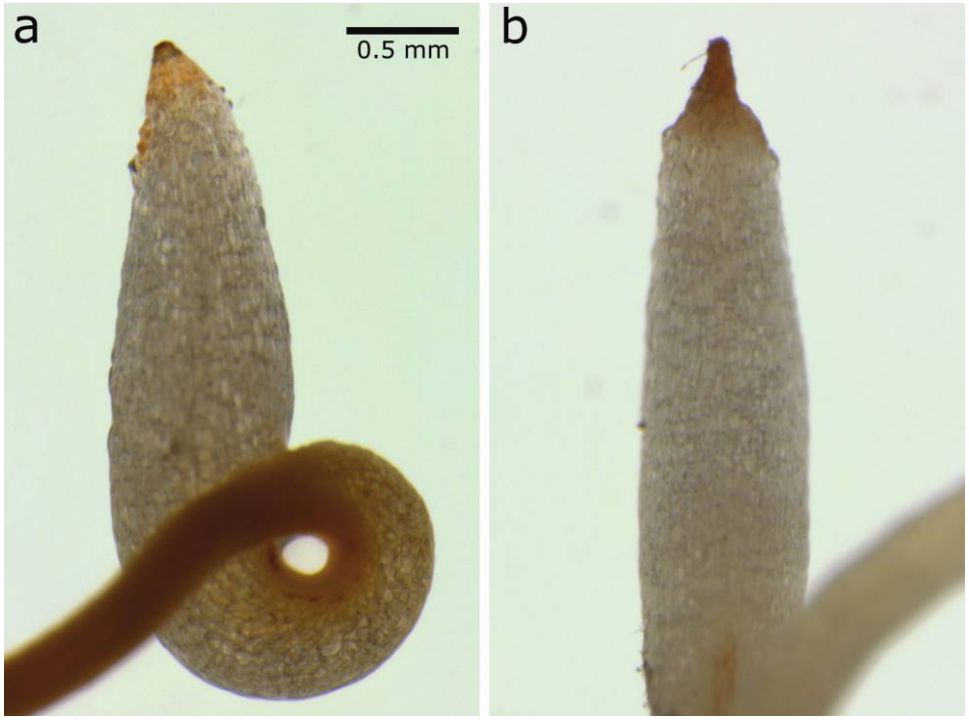

Fig. 1 Dodder seedlings after (*a*) ~2 and (*b*) ~7 d of growth. The younger dodder seedling shows the swollen root formation, whereas the older seedling shows signs of cellular collapse at the tip of the seedling.

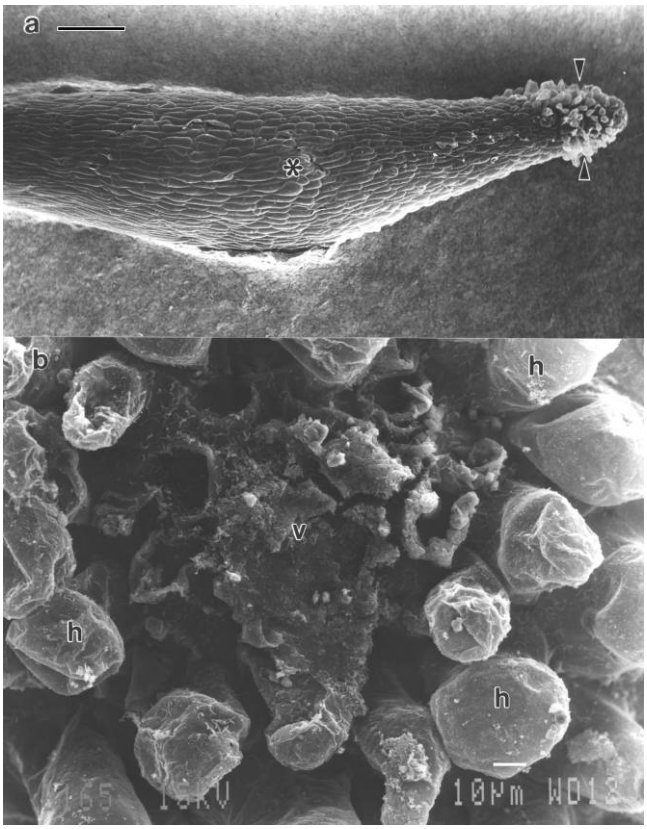

Fig. 2 SEMs of 3-d-old dodder roots. *a*, Relatively low magnification of the swollen region (asterisk) and the tip of the root (bracketed by arrowheads). *b*, Facing view of the root tip of the dodder tip of the dodder seedling. The vascular tissue (*v*) ends bluntly at the tip of the root and is surrounded by trichomes resembling root hair cells (*h*). Bars = 100 μm in *a* and 10 μm in *b*.

root, ending bluntly (figs. 2*b*, 3). Elements that appear to be developed or developing xylem or phloem tissue are found, although the tip area does not display the typical characteristics of a vascular cambium or a gradient of differentiated vascular elements. Rather, the tissues appear to be differentiated right up to the root terminus. The xylem elements (based on position and composition) seem to be simple, thin-walled cells devoid of cytoplasm and completely lacking the secondary-wall thickenings characteristic of most dicot seedling xylems. Root hairlike structures circle the terminus of the root, but they are irregular in morphology compared to the gently tapered root hairs found in other plants.

The 2–3-d-old root is much more swollen in appearance than a normally tapered dicot seedling root. The swollen nature of this tissue is most obvious when the relatively elongate cells in the 1-d-old root (fig. 3*a*) are compared with those in the 3–5-d-old seedling roots (fig. 4*a*), in which the cortical cells have expanded laterally to assume a more isodiametric shape. Plastids with prominent starch grains and nuclei are the most prominent organelles in the thin rim of cytoplasm that lies outside the large vacuole. Even in these relatively young 2–3-d-old roots, there is evidence of cell and tissue destruction, as crushed cells and cells with irregular wall formations are found. In none of the roots were there any indications of mitotic figures, although shoot meristem tissues at these same stages revealed numerous such figures.

Compared to the developing shoot tissue, the root tissue (with the exception of the vascular strand) is much less densely cytoplasmic than the shoot tissue (fig. 3*b*). These differences are obvious in all cell types, even the relatively undifferentiated epidermal cells. Moreover, there is little gradation of the effect but rather a dramatic difference between cells of the shoot and root zones. The shoot tissue is already starting its upward movement and is bent at near right angles in relation to the long axis of the root. The vascular tissue is continuous with the vascular tissue of the shoot, and there is little indication of any difference between the two at the shoot/root interface.

In later stages of root development (5–7 d after germination; fig. 4*a*, 4*b*), the cortical cells often appear degenerate, with evidence of extensive crushing and collapse of cells. Toward the tip of these degenerate roots, the cells appear completely empty

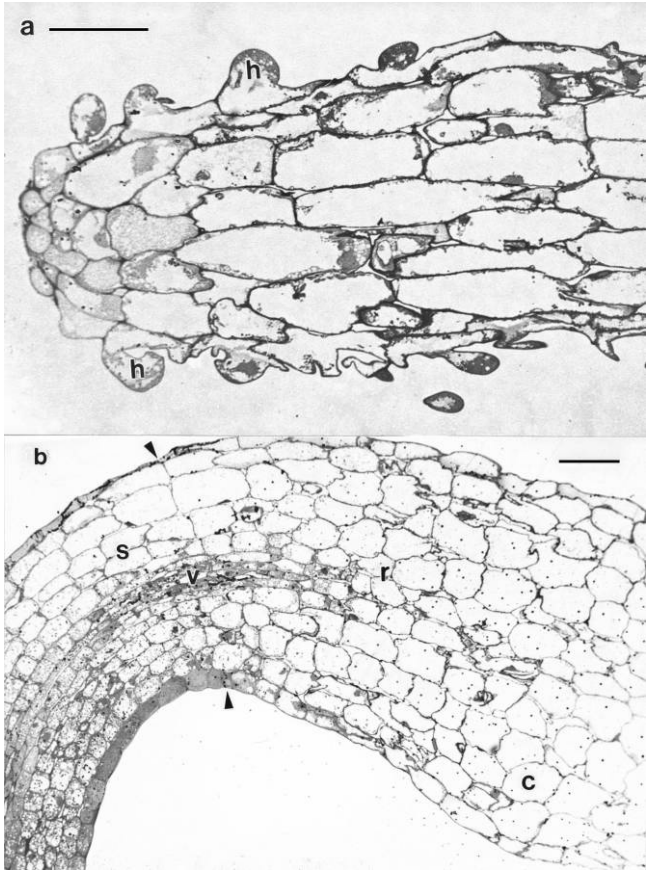

Fig. 3 LM sections of 1-d dodder root tip (*a*) and 2-d root/shoot intersection (*b*). Although the 1-d-old seedlings show relatively transverse cells and little swelling, by 2 d the cortical cells (*c*) are showing signs of swelling of the cells into more isodiametric cell shapes. At 2 d, the differentiation of the shoot (*s*) and root (*r*) tissue is easily apparent, with the denser cytoplasm and smaller cells of the shoot tissue compared to the root. Vacuoles of the epidermal shoot tissue display more opaque contents than those of the root. Arrowheads mark the separation between root and shoot. *v* = vascular tissue; *h* = hair cells. Bars = 50 μm in *a* and *b*.

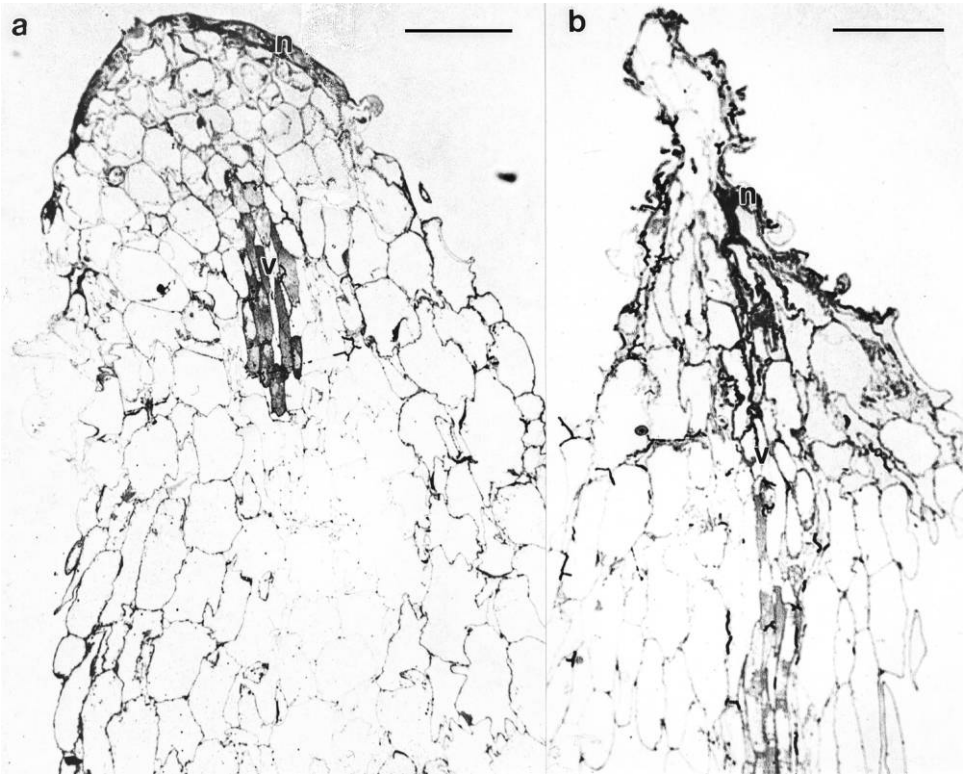

Fig. 4 LM sections of (*a*) 5- and (*b*) 7-d dodder seedlings. *a*, At the tip of the root end of the 5-d-old seedling, necrotic cells (*n*) are found chiefly along the edges of the tissue, with the vascular tissue remaining relatively intact despite the swollen necrotic cells all around. *b*, In the 7-d-old root tissue, the entire tip of the seedling is necrotic (*n*), with the massive collapse of all the cells. Cells in the vascular region (*v*) are the most normal. Bars = 100 μm.

of contents and have an overall strong reaction with toluidine blue, perhaps an indicator of released phenolic compounds from the vacuole or residual membranes from destroyed organelles. The vascular strand appears to be the one area of cells that persists at this stage of degeneration (fig. 4*b*). In some of the roots, the epidermal cells near the tip and hairs appear to degenerate first. These form a collar of degenerate cells at the tip. In other roots, subepidermal and epidermal cell degeneration occurs, apparently simultaneously.

Electron Microscopy of Young Root Tissue

In the very young (1–2-d-old) dodder root, the cytoplasm of the cortical cells reveals a very distinct ultrastructure (figs. 5–7). Nuclei in these cells are prominent and, in contrast with nuclei in shoots, are distinctly larger (×2–×4 in cross section) and contain extensive cytoplasmic invaginations or inclusions that produce a distinctive wavy outline (fig. 5*a*). Often, chromatin patches were found around these invaginated areas of the nuclear envelope. The larger size of the root nuclei relative to those in the shoot may be indicative of endopolyploidy of these cortical cell nuclei. Supporting this idea of endopolyploidy is the incorporation of bromodeoxyuridine into these nuclei (indicating new DNA synthesis), despite the lack of mitotic figures (not shown).

Plastids (fig. 5*b*) are similar in ultrastructure to those noted previously in shoot tissue despite the visibly less green or yellow aspect to the root tissue compared with the shoots. Thylakoids are arranged mostly in doublets. In addition to the prominent starch grains, several sorts of less typical inclusions (crystals, phytoferritin) are also commonly found. The cytoplasm has a high density of ribosomes. Golgi and ER (and a number of vesicles probably derived from one or the other of these) are found abundantly throughout the cytoplasm (fig. 5*c*).

Cell walls of cortical cells in the very young dodder roots display a close relationship between the arrangement of cellulose microfibrils and the cortical microtubule array (fig. 6*a*). However, no mitotic, preprophase or phragmoplast microtubule arrays were noted using methacrylate sections probed with antitubulin antibodies (not shown) or in TEM sections. Prominent osmiophilic particles, associated with wall loosening, are found both in the walls themselves and are associated with the cortical cytoplasm and microtubules (fig. 6*c*). Cortical epidermal cells and root-hair cells contain a thin (~0.1 μm) cuticle (fig. 7*d*) that coats the surface of the tissue, similar to that found in shoot tissue. Root hairs, even at this early stage, are not elongate as in root hairs of other dicot species but instead are abnormally shaped and contain relatively little cytoplasm or organelles. SEM reveals the three-dimensional distribution of these hairs, which are clustered very near the end of the root tissue (fig. 2*a*, 2*b*), forming a wreathlike structure. The blunt, scarlike end of the vascular tissue is also obvious as a circle of cells at the root center in these micrographs (fig. 2*b*).

Cells in the vascular tissue displayed much of the same internal structure as the early cortical cells with the exception that

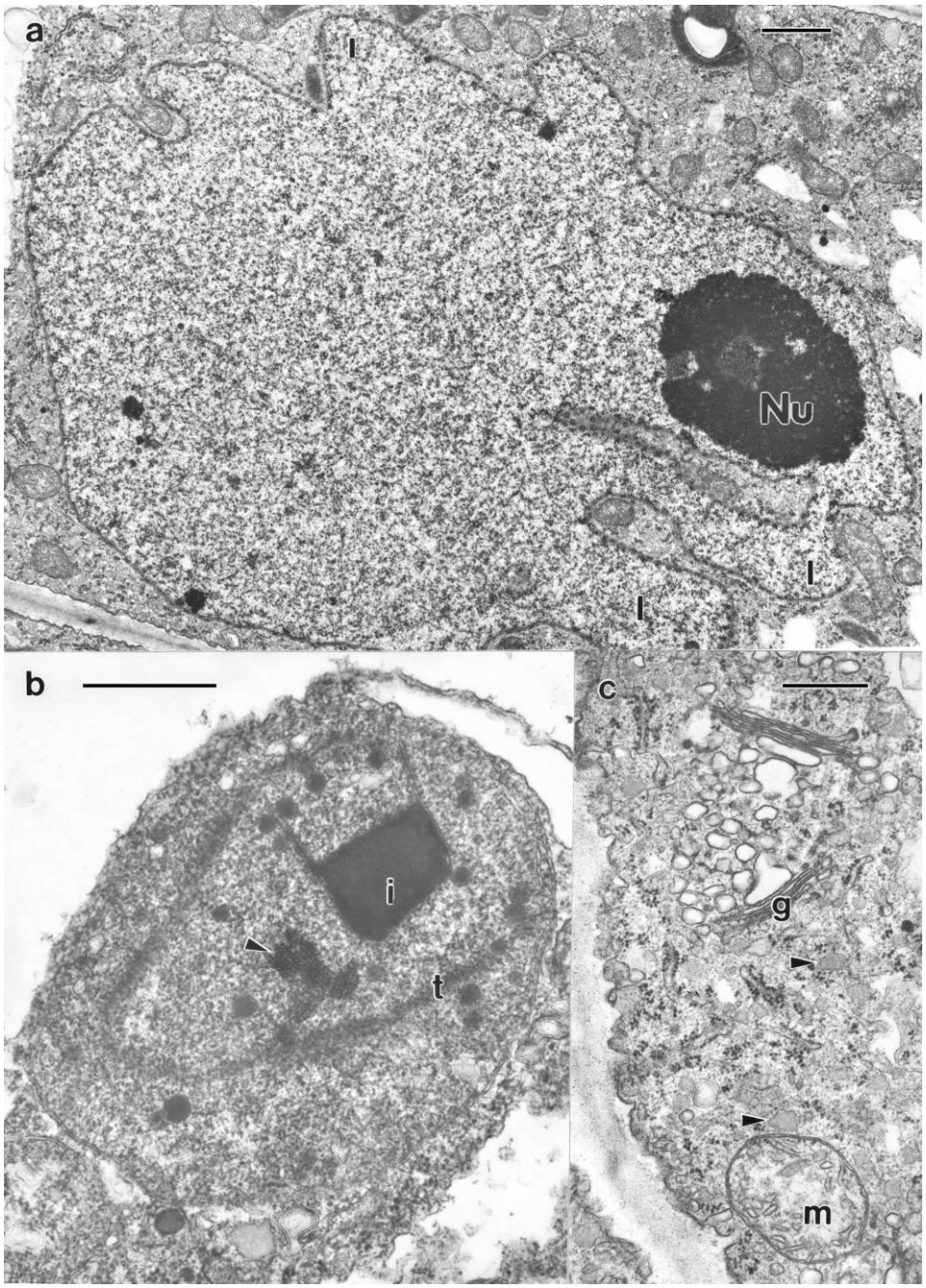

Fig. 5 Electron micrographs of 1-d-old dodder seedlings. *a*, The nucleus of the root cells is distinctly lobed (*l*) and three to four times the size of nuclei in shoot tissue of these same seedlings. *N* = nucleolus. *b*, Although the root tissue is colorless or nearly so, plastids in these tissues are similar to those found in shoot tissue of dodder. A prominent inclusion (*i*), a crystal (arrowhead), a rudimentary thylakoid system (*t*), and phytoferritin aggregates are noted. *c*, The cytoplasm of the root cells at 1 d after germination is very rich with electron-translucent Golgi vesicles and other vesicles that presumably contain hydrolytic activities. *g* = Golgi apparatus; *m* = mitochondrion. Bar = 2 μm in *a*, 0.5 μm in *b* and *c*.

the vascular parenchyma tissue also has prominent structures that are thought to be actin bundles (fig. 6*b*) that run the length of these long cells. Even toward the root tip, cells that are typical of differentiated sieve tubes and simple xylem vessels are noted. However, the xylem elements have just a thin primary wall rather than an elaborate secondary wall found in most dicot roots. Sieve elements do not have typical wall ingrowths, and no P protein crystals were noted in these elements (fig. 7*b*, 7*c*). The sieve elements do have characteristic sieve-type plastids, aggregates of smooth ER, mitochondria with swollen cisternae, and callosic swellings at the sieve plate, however. Although root tissues of typical dicot seedlings have a pericycle and a Casparian strip, neither pericycle nor Casparian strip were found around the vascular tissue in the dodder root.

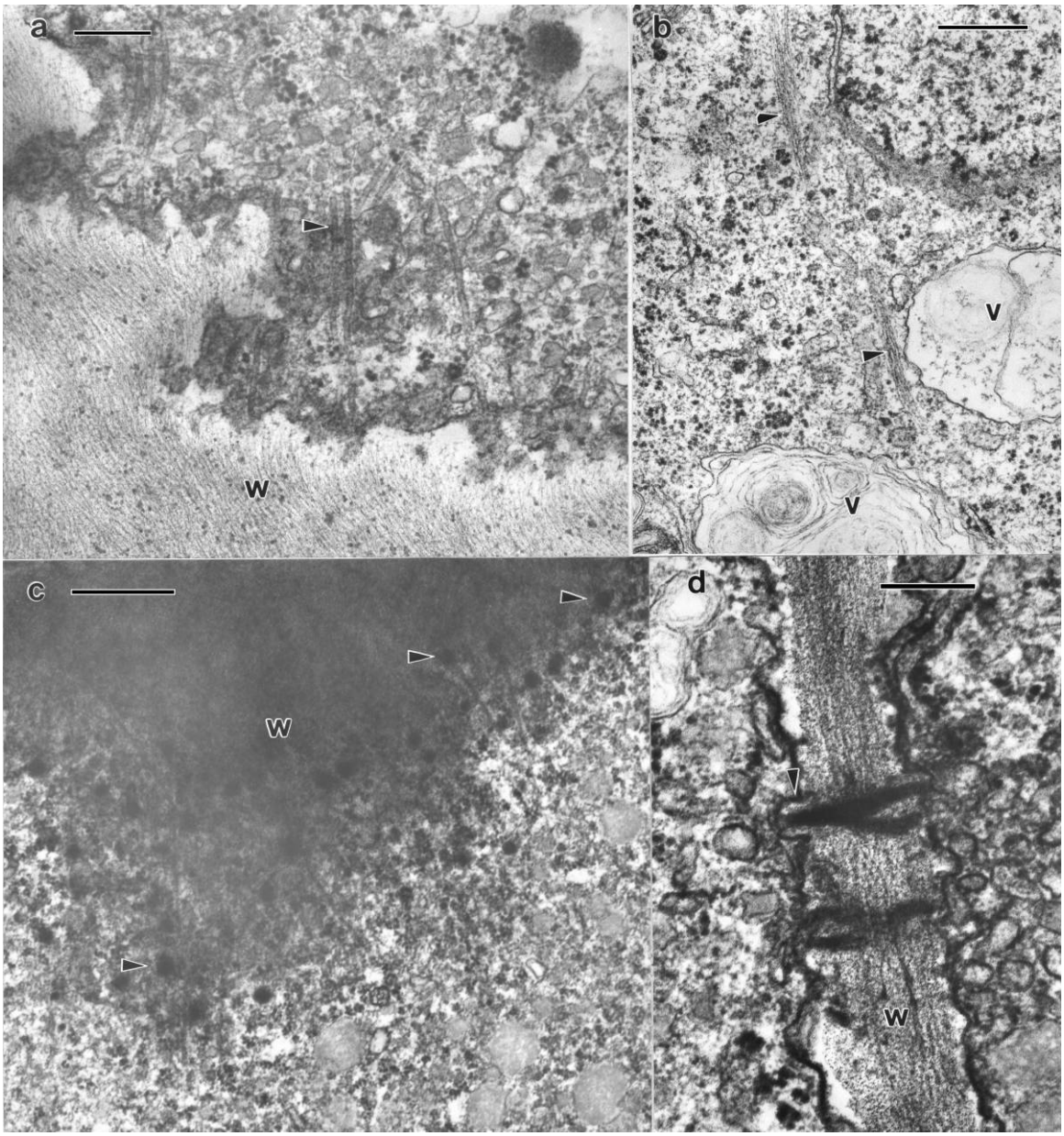

Fig. 6 Electron micrographs of walls and cytoskeletal elements in 1-d-old dodder seedlings. *a*, Microtubules (arrowheads) are prominent in the cytoplasm of the 1-d-old dodder seedling, and their orientation is parallel to that of the cellulose microfibrils in the cell wall (*w*). *b*, Actin microfilaments (arrowheads) are found as threadlike complexes running through the cytoplasm and are especially prominent in vascular parenchyma cells such as this one. Small vacuoles (*v*) that appear to be lytic in function are also prominent in these cells. *c*, Osmiophilic particles (arrowheads), associated with cell-wall loosening, are found prominently in this oblique section of cell wall (*w*). The position of some of the osmiophilic particles is suggestive of a microtubule orientation of these particles in the cell wall (*w*). *d*, Plasmodesmata are often found connecting cells in the 1-d-old dodder seedling, but the usual electron-translucent collar around the plasmodesmata is not apparent. However, there are protrusions of the cell wall (*w*; arrowhead) around the termini of the plasmodesmata. Bars = 0.2 μm in *a* and *d*, 0.5 μm in *b* and *c*.

Electron Microscopy of Older Dodder Roots

In 3–5-d-old root tissue (fig. 8), there is a progressive deterioration of all of the cortical tissue similar to senescence or apoptotic events described in other plant systems. Cytoplasmic organelles appear degenerate. These changes may be induced by a loss of integrity of the tonoplast membrane and the plasmalemma–cell wall connection (fig. 8*c*, 8*d*) so that cellular fluids leak from the cell, resulting in severe osmotic changes. In some cases, organelles are engulfed by lytic vacuoles (fig. 8*c*). The nuclei in the cortical cells of the older dodder roots are highly lobed, and chromatin is clustered near the nuclear envelope as in apoptotic degradation described in other systems. Thus, virtually all the cytoplasmic organelles exhibit the characteristic morphology of senescence or apoptosis.

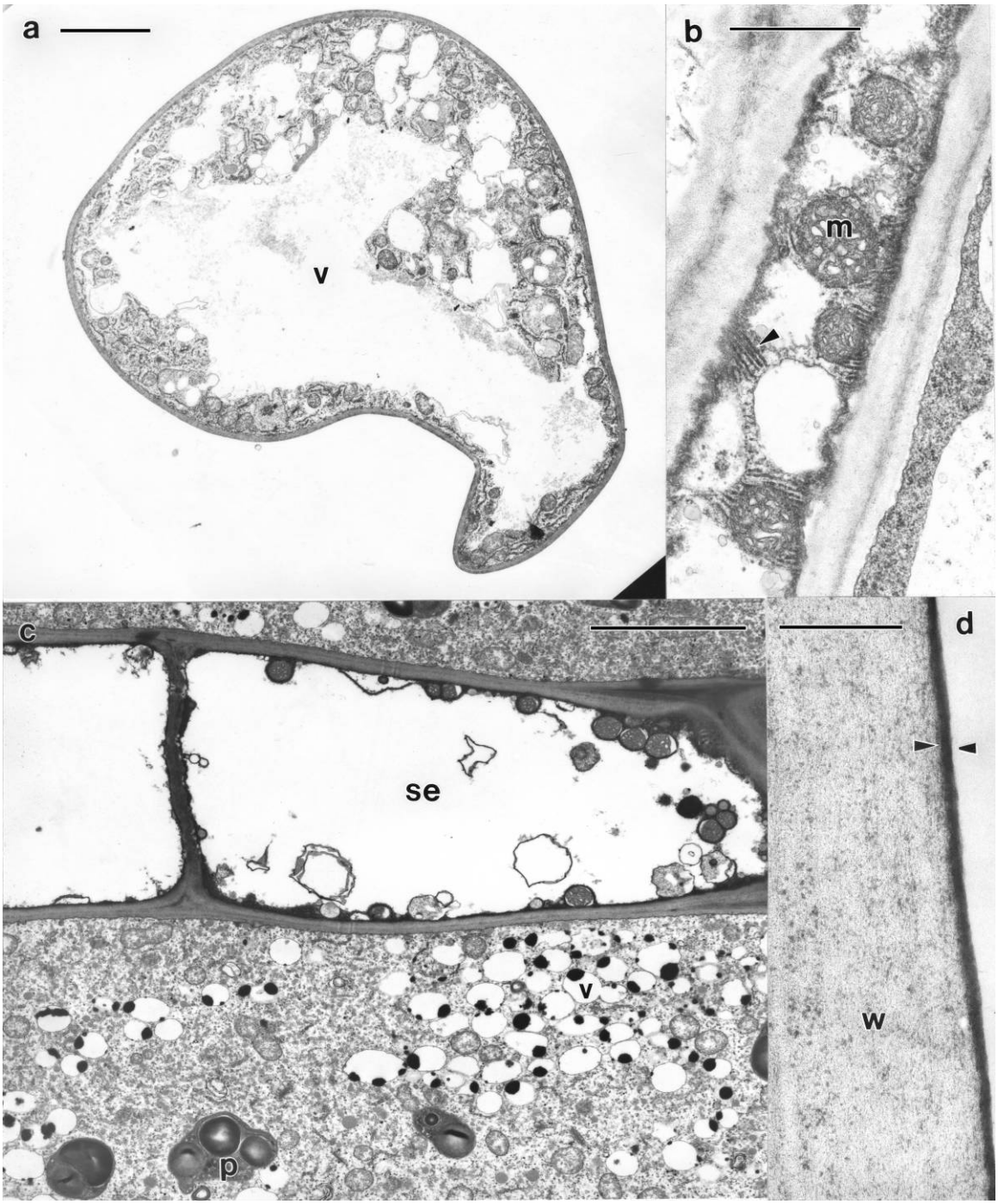

Fig. 7 Electron micrographs of epidermal (*a*, *d*) and vascular (*b*, *c*) tissue in 1-d-old dodder roots. *a*, Root hairs of dodder seedlings are irregularly shaped cells that contain the same sort of organelles found in root hairs, but their distribution reveals less tip growth than in root hairs of other species. A prominent vacuole (*v*) occupies the central area of the hair cell. *b*, An edge of a sieve cell, with prominent mitochondria (*m*) and microtubules (arrowhead). *c*, Low-magnification micrograph revealing the well-developed sieve elements (*se*) immediately adjacent to the densely cytoplasmic cortical cells. Small vacuoles (*v*) in the parenchyma cell may have electron-opaque storage compounds. *p* = plastid. *d*, The wall (*w*) of an epidermal cell of dodder displays a prominent electron-opaque cuticular layer (bracketed by arrowheads). Cuticles are not present on roots of most species. Bars = 2.5 μm in *a* and *c*, 0.2 μm in *b* and *d*.

Unlike the highly organized wall structure found in the younger dodder roots, in older dodder roots, there are few organized cellulose microfibrils, few cortical microtubules, and a high number of osmiophilic particles, which are thought to be associated with wall loosening. Thus, the absence of cortical microtubules to direct the location of new-wall synthesis and the presence of cell-wall-loosening factors cause the cells to swell against an increasingly less resistant cell wall. Besides

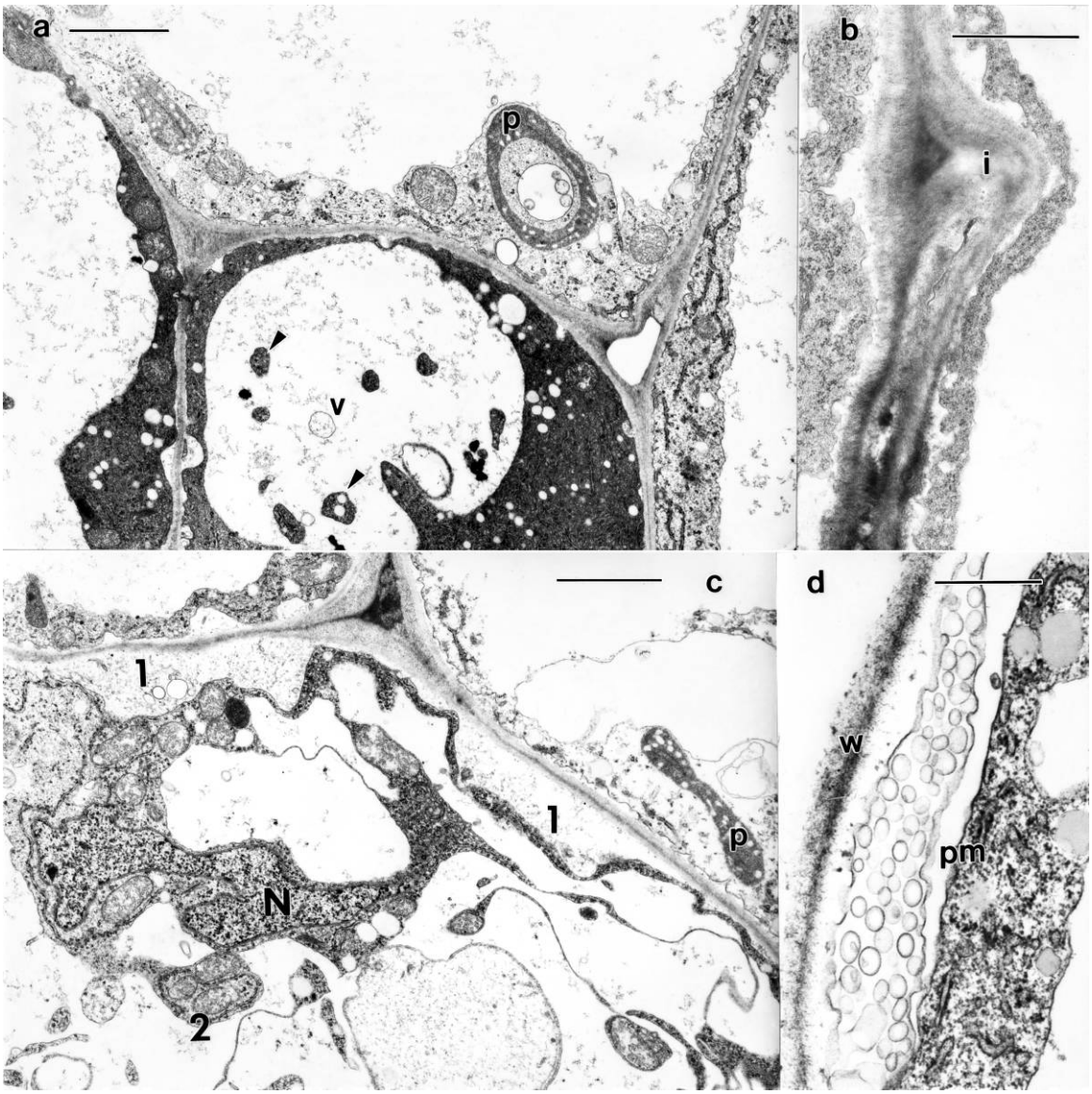

Fig. 8 Process of cellular degeneration in dodder root cells in 3–5-d-old dodder seedlings. *a*, Low-magnification electron micrograph of a 3-d-old root with cells of various cytoplasmic densities. A vacuole (*v*) in one cell contains membrane fragments and pieces of engulfed cytoplasm, indicative of autophagy. *p* = plastid. *b*, A small wall ingrowth (*i*) caused by the expansion of neighboring cells. *c*, In this cell, detachment of the plasmalemma from the primary wall is marked *1*, and the segmentation of the cytoplasm and engulfment of organelles is marked *2*. A portion of a very lobed nucleus (*N*) is apparent. *p* = plastid. *d*, In a 5-d-old dodder seedling, the wall (*w*) and the plasma membrane (*pm*) are detached, with an abundance of vesicles and membrane fragments between these structures. Bars = 2.0 μm in *a* and *c*, 1.0 μm in *b*, and 0.5 μm in *d*.

causing massive changes in its own position, the swelling of one cortical cell puts increased pressure on the surrounding cells, leading to cellular collapse and contorted cell wall formations throughout the tissue. This massive cell wall loosening and subsequent expansion of the cells probably accounts for the swollen, clublike morphology of the young dodder root and its subsequent collapse at later stages.

As noted in the LM sections, tissue in the vascular strands remain mostly intact despite the massive changes that are occurring in the cortical cells. These maintain their integrity even in tissues where the nearby cortical cells are collapsed and free of cytoplasmic contents. The electron opacity of the cytoplasm in vascular tissue from older roots is greater, but this may be due to a release of phenolic compounds from the neighboring senescent cortical cells, as the changes appear similar to what happens when tannins are added to the fixative.

Immunocytochemical Characterization of the Dodder Walls

Because many of the structural characteristics of the dodder walls are unusual, we probed semithin sections of mature (day 2–3) but not yet visibly senescent dodder roots with a battery of antibodies to determine the presence and distribution of

various polysaccharides (figs. 9, 10). Antibodies that recognize rhamnogalacturonan I (RGI) or pectic mucilages (CCRC-M38, -M22, -M10), highly de-esterified homogalacturonans (JIM5), and arabinogalactan proteins (AGPs; CCRC-M7 and JIM13) reacted strongly with the root segments. All cell types were labeled, although the root hairs were relatively less so than other cell types. In contrast, two side chains of RGI, recognized by LM5 (1→4 galactan side chain) and LM6 (1→5 arabinan side chain), labeled only the hair cells (LM5; not shown) or displayed a gradient of labeling from weak at the tip to progressively more strong as the cells approach the shoot (fig. 10). The same pattern seen with LM6 was also noted with the pectic mucilage antibody CCRC-M34 and the highly esterified homogalacturonan antibody JIM7 (fig. 10). No reaction was noted with the CCRC-M1 antibody that recognizes fucosylated xyloglucan (not shown), although this antibody has recognized xyloglucans in every plant tissue (with the exception of the Solanaceae) for which we have used this particular probe. Similarly, the LM10 and LM11 antibodies, which have labeled xylem wall ingrowths in all tissues previously surveyed, including dodder shoots and xylic hyphae, failed to label the thin-walled xylem/protoxylem of the dodder roots (not shown).

We also performed a series of studies on sections of plants embedded in epoxy resin and thin-sectioned at ~100 nm. The standard immunocytochemical technique is to use acrylic resins, such as LR white, because their increased porosity allows the antibodies better access to the antigens in the sections and they require less time and lower temperatures for polymerization. However, we have found that, perhaps due to their relative size (compared with proteins) and high concentration into the cell walls, some polysaccharides can be detected when embedded in epoxy, which better preserves ultrastructural detail than acrylic resin. Unfortunately, not all of the antibodies used above reacted well with these sections, but a number of polyclonal sera and the cellulase-gold probe did. This also allowed a quantitative analysis of some of the changes in antibody labeling over time in tissue blocks that we had examined for structure. In each case, parenchyma cells adjacent to the vascular tissue near the

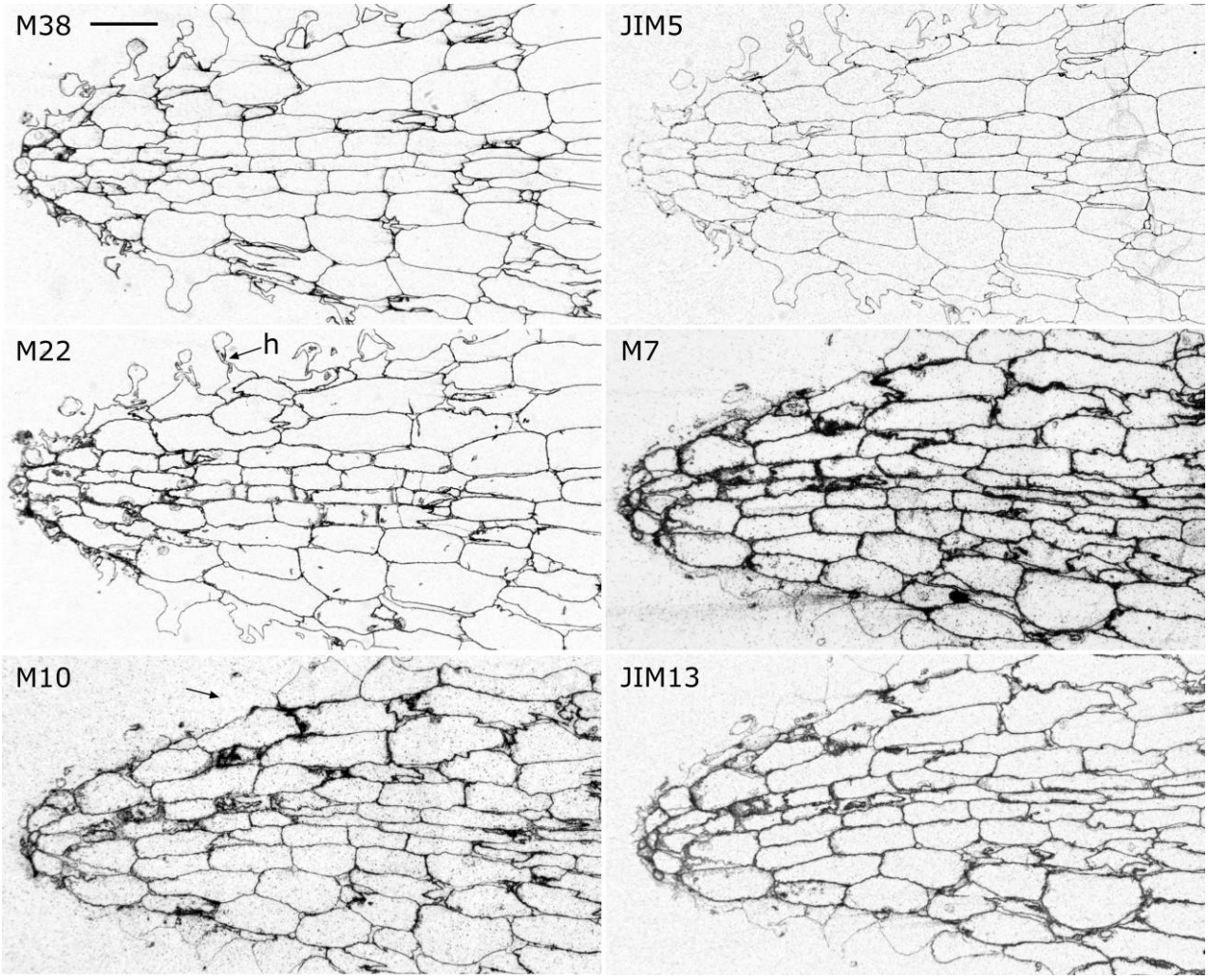

Fig. 9 Immunogold-silver localization of polysaccharides in young (1–3-d old) roots with a variety of pectin (CCRC-M38, -M22, -M10, and JIM5) and AGP (CCRC-M7 and JIM13) antibodies. Other than some lighter or patchy staining of the "root hairs" (*h*), each of these antibodies labels all of the walls and relatively equally. Bar = 100 μm.

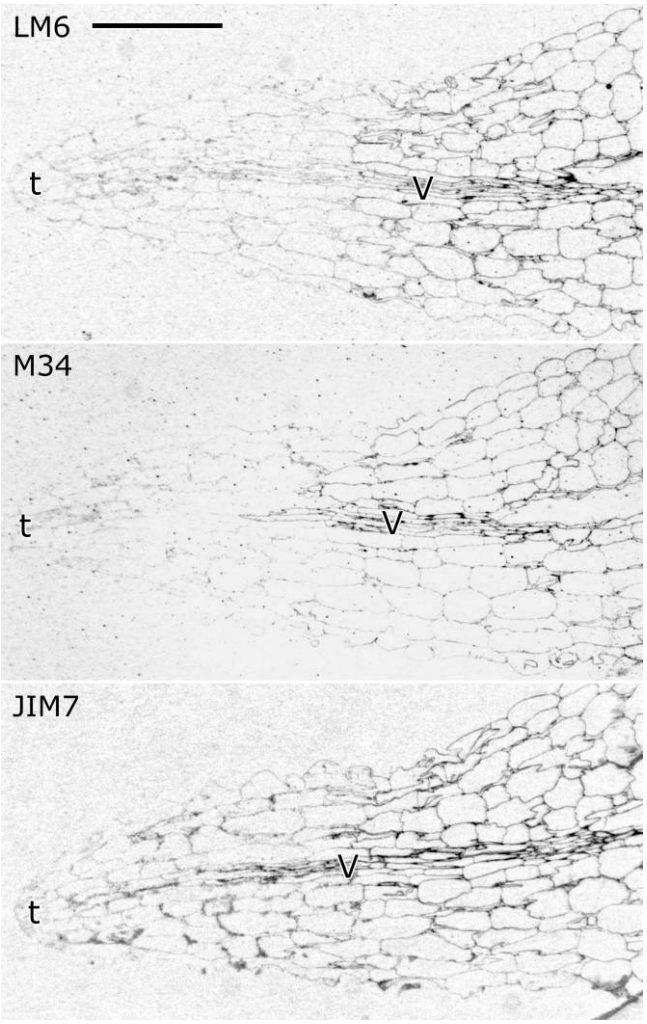

Fig. 10 Immunogold-silver localizations of three different pectin epitopes on dodder roots. JIM7 recognizes highly esterified homogalacturonans, CCRCM34 recognizes pectic mucilages, and LM6 recognizes the 1→5 arabinan side chain of RGI. Unlike the pectic epitopes monitored in fig. 9, each of these epitopes reveals reduced labeling at the tip (*t*) of the dodder root with enhanced labeling at sites away from the tip and along the vascular tissue (*v*). Bar = 1 mm.

tip of the root were chosen so that temporal rather than spatial differences would be monitored. When 1-d-old dodder roots are probed with antisera to polysaccharides, a labeling pattern very typical of dicot cell walls is noted in the root tissues. Cellulose affinity probes, xyloglucan antisera, and antibodies to esterified pectins strongly label the wall matrix (table 1). Antibodies to primarily de-esterified pectins label the middle lamellae, and those to callose label the plasmodesmata, with relatively little in the wall per se. In contrast, the older, more swollen roots are labeled much less with the cellulose probe and the xyloglucan antibodies but strongly with antibodies to both esterified and de-esterified pectins (table 1). These data indicate that the walls of the cortical cells are being degraded/chemically altered during the swelling of the dodder root, with the normal matrix material being replaced by pectins; it is also possible that the loss of cellulose has exposed previously buried epitopes of pectin. Although one might expect callose levels to increase markedly as a result of a wounding-type response associated with the degradation of the cortical cells, no substantial change in callose immunolabeling was noted, despite large changes in cell-wall/plasmalemma continuity. Quantification of the immunogold and affinity-gold labeling reveals that only 20%–30% of the density of cellulose and xyloglucan label was detected in 5-d-old dodder roots compared with 1-d-old seedlings. There is an increase by ~40%, however, in the labeling of de-esterified pectins in the walls on a square-micrometer-of-wall basis (table 1). This increase could be due to new synthesis, the uncovering of buried pectin epitopes that are exposed because of cellulose loss, and/or the de-esterification of existing esterified residues. These data indicate that loosening and degradation, as well as compositional differences in the wall, accompany the changes in morphology of cortical cells of dodder root.

Biochemical Changes Associated with Dodder Roots

Biochemical and immunochemical comparisons of shoot and root protein extracts also indicate an abnormality in cytoskeletal proteins in root extracts. When separated electrophoretically, total homogenates of root and shoot tissues are similar in that the intensity of banding on the gel is comparable, but the profiles are markedly different (fig. 11). Western blots probed with well-characterized monoclonal antibodies to actin and α-tubulin reveal single strongly labeled polypeptide bands at 43 and 55–56 kDa, respectively (fig. 11). In contrast, the extract from root tissue gives only weakly labeled bands with any of the tubulin antibodies. However, extracts of onion roots, which were used for comparison, showed strong labeling for both tubulin and actin (fig. 11). Thus, tubulin protein is present in quantities that are much lower in the roots compared with the shoots on a total protein basis and in relation to the quantities of actin within the root. Whether these changes in tubulin protein level set into motion the subsequent changes in cell wall morphology or whether the tubulin levels are a consequence of other senescent/apoptotic events is not known. Certainly, there is a very close relationship between the integrity of the walls and the presence of cortical microtubules.

Table 1

Quantification of Immunogold and Enzymogold Labeling of Dodder Root Walls during the Breakdown of the Wall Structure

	Root age		
Probe/antibody	1 d	3 d	5 d
Cellulase-gold	74	44	22
JIM7 (esterified pectins)	49	51	69
JIM5 (de-esterified pectins)	6	16	27
PGA polyclonal	8	18	20
Xyloglucan polyclonal	87	77	22
Callose monoclonal	6	8	6

Note. Data are expressed in gold particles μm^{-2} of wall area not inclusive of either plasmodesmata or middle lamellae. Data are the averages from at least three sets of experiments and are rounded off to the nearest whole integer.

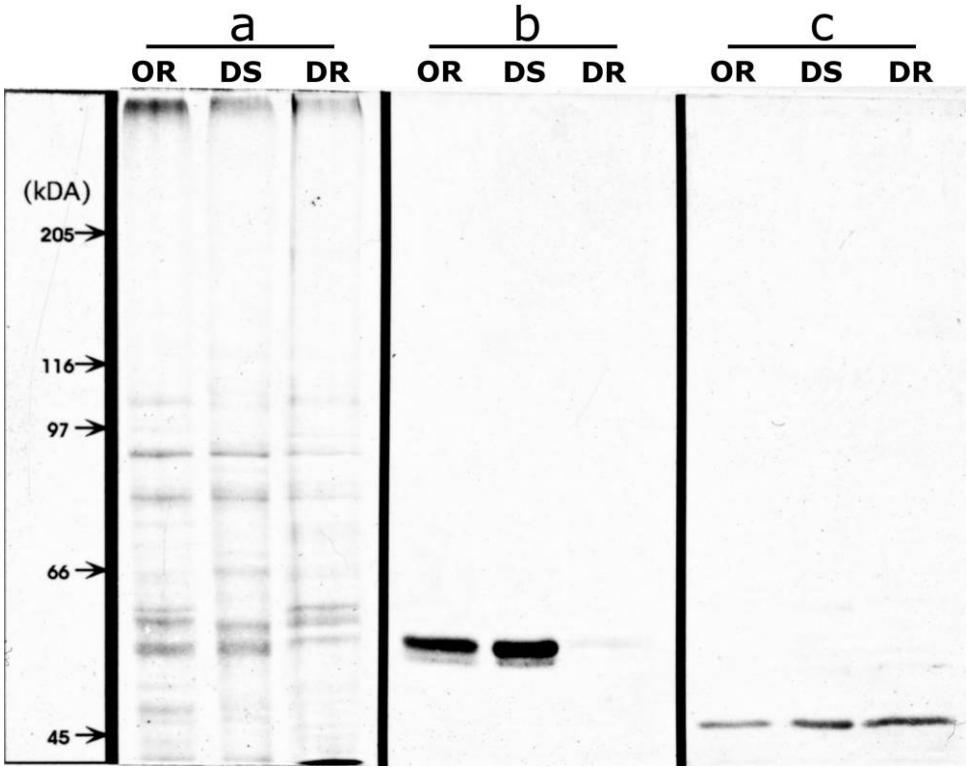

Fig. 11 Acrylamide gel stained with Coomassie blue (*a*) and Western blots (*b*, *c*) of roots and shoots of dodder and roots of onion. Protein profiles of the root and shoot extracts are distinctly different. Blots probed with α tubulin (*b*) reveal much stronger labeling in the shoot extracts than the roots, whereas actin blots (*c*) reveal essentially equal labeling on a protein basis. *OR* = onion root, *DS* = dodder shoot, *DR* = dodder root.

Because the nuclear morphology of the root indicates a possible apoptotic mode of tissue degeneration, attempts were made to determine if DNA laddering, typical of apoptosis, was noted. However, DNA profiles were smeared and not laddered (not shown).

Discussion

Dodder Root Lacks Many Features of Other Dicot Seedling Roots

In many respects, the tuberous end of the dodder seedling has the appearance of a root (fig. 1). However, there are many features typical of root tissues that are not present in the dodder root. Dodder roots lack root meristems (calyptyrogen, apical, and vascular cambium). Instead, well-differentiated vascular tissue ends bluntly at the root terminus (figs. 2–4). Cells resembling root hairs (fig. 2) are found in a zone that would be roughly comparable to the position of normal dicot roots if the dodder root had both an apical meristem and a cap. However, the dodder root hairs are irregular in shape compared with the root hairs of dicot seedlings and do not show the same abundance or placement of organelles typical of this cell type (figs. 2, 7), and they only occur in a narrow band toward the root tip. Moreover, the entire root is covered with a cuticle of similar thickness to that in the shoot tissue (fig. 7*d*). If the purpose of the root tissue is absorption of water, a waxy cuticle around the root is counterproductive, as this would prevent rather than enhance water uptake.

Vascular strands in roots are distinguished from those in shoots by the presence of a pericycle and a Casparian strip (Evert 2006), a band of suberized tissue that surrounds the vascular strand. There is, however, no pericycle or Casparian strip surrounding the vascular tissue in the dodder root. Thus, a defining characteristic of roots in general is missing from dodder roots. Even within the vascular strand, the vascular elements are rather primitive. The phloem cells lack P protein, and the xylem cells are identifiable as such only in that they lack a protoplast and are found in the vascular strand. No secondary walls, xylans, or lignins are found in these root xylem elements even though both stem xylem and xylic hyphae have been shown to have these same constituents (Vaughn 2006). Lyshede (1986) made a similar diagnosis of these empty cells as xylem in another dodder species. Moreover, the dodder roots do not respond to the normal geotropic signals that other roots do, nor do they even penetrate the fine and relatively porous potting mix that was used in our previous studies (Vaughn 2003). In an embryological study, Truscott (1966) found no evidence for root tissue but did identify some dead cells at the tip of the seedling axis that may have been degenerate root tissue progenitors. That data would also indicate that the zone of the root occupied by root hairs is not a root remnant either.

Clearly, the tuberous end of the dodder seedling is differentiated from the shoot tissue. These differences include that (1) the cells contain a much lower density of organelles (fig. 3), (2) the tissue is swollen and not elongate (figs. 1–3), (3) the tissue is white compared with the yellow-green shoot (Sherman

et al. 1999), (4) the cortical cells are much larger and more vacuolate than those of the shoot (fig. 3), and (5) the nuclei are large and highly convoluted and probably endopolyploid (fig. 5*a*). The lack of so many other characteristics of root tissue summarized above indicates that the tuberous region of the dodder seedling should probably be considered a highly modified shoot end. This rootlike tissue serves as an anchor for the dodder seedling and a reserve of nutrients that can be assimilated before the seedling achieves a parasitic union. Lyshede (1986) reached a similar conclusion in his study of the dodder root, prompting him to refer to this structure as a "tuberous radicular end."

Dodders are unique among vining plants in that the seedling germinates directly into the vining mode (K. C. Vaughn, unpublished observations). Other vines, including those in the once lumped and probably closely related Convulvaceae, germinate as a nonvining herbaceous seedling and then convert to the vining mode in third or fourth nodes (K. C. Vaughn, unpublished observations). In these other vines, the first few nodes of the seedling serve as a sort of anchor for the subsequent vining form. It may be that the swollen rootlike structure found in dodder serves a similar anchoring function.

Why Do the Dodder Roots Swell?

Mutations, chemical treatments, and even natural occurrences cause tissue swelling or "radial expansion" (Baskin et al. 1992, 1994). When roots of young seedlings of other species are treated with microtubule disrupters such as colchicine or oryzalin, the root tips swell into a clublike structure (Hoffman and Vaughn 1994). This is the result of cells in the zone of elongation swelling laterally rather than elongating, and this is due to the lack of cortical microtubules and an increase in the size of cells attempting to divide but failing because of a lack of spindle microtubules. The change from cell elongation to lateral swelling causes this gross morphological shift from elongate to clubby roots. Seedlings exposed to compounds that disrupt other cytoskeletal components (Baskin et al. 1994) and cellulose biosynthesis (Vaughn 2002*b*) also swell, either through secondary effects on the microtubules or through reduced wall strength allowing osmotic swelling.

The clubbing of the dodder root tissue is probably the result of several different mechanisms. The cortical cells of the root tissue do change in morphology from elongate cells in the 1-d root to much less elongated, swollen cells even after only a second day of growth. Similarly, cortical microtubules are much less abundant after several days postgermination, which would affect the ability of the cell to maintain the elongate shape. In addition to the cytoskeletal changes, the walls of these cells change compositionally from the normal cellulose-xyloglucan walls with cellulose microfibrils to cells composed of more pectin (table 1), and even there the RGIs have lost their side chains (figs. 9, 10). The addition of wall-loosening complexes or osmiophilic particles that contain the protein expansin (Vaughn et al. 2001) also occurs during this time and would allow for significant slipping of the cellulose-xyloglucan linkages. Recently, Schoenboek et al. (2007) have shown that treatment of dodder seedlings with a glucuronidase inhibitor affected root swelling (fig. 6 in that article). Thus, the wall-loosening effects must be critical for the swelling to occur. From these data, the swelling of the roots of dodder is probably due not only to the loss of cortical microtubules but also to the weakening of the wall, allowing the internal cellular pressures to expand the cortical cells.

Is Senescence or Apoptosis Involved in the Degeneration of the Dodder Root?

Plant cells and tissues end their existence either through a programmed cell death (e.g., xylem element formation) or through a senescence-like process (e.g., fruit ripening). The data in this study indicate that the loss of integrity of the dodder root is more like a senescence event than apoptosis, although elements of apoptosis may also occur.

Changes in nuclear morphology, especially the highly lobed nuclear envelope and the clustering of chromatin at the nuclear envelope (fig. 5*a*) are classic indicators of apoptosis. It should be noted, however, that nuclei from clearly nonsenescent or nonapoptotic cells may also exhibit this morphology (Collings et al. 2000). Furthermore, we were unable to detect significant DNA laddering in DNA isolated from root tissue (this study). A similar sort of cell-specific degeneration has been described recently for aerenchyma formation in the roots of maize (Gunawardena et al. 2001*a*, 2001*b*). These researchers found that although the ultrastructural indicators of apoptosis were present, DNA laddering was relatively minor even in tissues in which extensive apoptotic events were detected by electron microscopy. The absence of laddering is probably reflective of asynchronous death, in which a small portion of cells are destroying DNA at a given instant rather than the massive and simultaneous alteration to DNA that occurs in some animal tissues undergoing apoptosis. There are other parallels between the cortical cells of dodder roots and those of maize root aerenchyma. In both dodder roots and maize aerenchyma, organelles are degraded, there is a large increase in cell volume, and the walls are loosened with a concomitant increase of pectins in the cell walls. Dodder cortical root cells complete this process by a total degeneration of the tissue, which is more akin to true senescence (unlike in aerenchyma of maize), but otherwise the parallel between the two systems is striking.

In ripening fruit, the loss of the side chains of RGI is an early event in the process (Pena and Carpita 2004). In the dodder root, LM6 and LM5 labeling (both of which recognize side chains of RGI) is lost from the cell walls, even though the roots still have integrity (fig. 10). Moreover, homogalacturonans, such as those recognized by JIM7, are also lost from the walls. Interestingly, these homogalacturonans have also been implicated as being side chains of RGI (Vincken et al. 2003). This loss does not imply an absence or modification of all pectins, however. Antibodies to the pectin backbone and mucilaginous pectins (probably also recognizing debranched RGI epitopes) strongly label these young roots, indicating that the side chains have been lost but not the parent molecule. This observation agrees with that from fruit ripening and is consistent with the hypothesis that the roots are undergoing senescence rather than apoptosis. Bowling and Vaughn (2008) observed a similar loss of RGI side chains in papillate cells of Virginia creeper tendrils and a commensurate strong reaction with antibodies that recognize RGI without side chains and

pectic mucilages. Thus, in another type of vine, a similar process occurs in cells that will die relatively soon after their function has been performed.

Treadmilling and the Sustenance of the Dodder Seedling

During the relatively short time period covered in this series of experiments, the root of the dodder seedling rapidly transformed from a newly germinated healthy organ to one with little integrity. Because dodder seedlings have no cotyledons and very little chlorophyll from which to derive photosynthetic energy (Sherman et al. 1999), the seedling must be sustained by internal reserves before a successful parasitic union is formed. One area that could store such reserves without affecting the viability of the plant is the root end of the shoot. Plastids, for example, contain large amounts of starch (and lipids and proteins) that could be metabolized, transported, and then utilized later in shoot sustenance. Lee (2007*b*) described a similar sort of storage material in vacuoles of embryos and subsequent breakdown in order to sustain young seedlings of dodder. The demise of the cortical tissue (figs. 1, 4), starting most prominently with the very tip of the root, would allow these reserves to be channeled to the fast-growing tip. Moreover, the retention of the vascular tissue even when all other tissues are destroyed would allow a conduit for the movement of such reserves to the shoot portions of the tissue. A similar gradient of terminal degradation is seen within dodder shoots such that the lower portions of the stem go through senescence or programmed cell death to sustain the growing tip (Lyshede 1989). Thus, one could envision the growing dodder seedling as sort of a treadmill. At the root end, it is being degraded in order to sustain the growth of the quickly expanding shoot tissue. As shown by the growth data described above, the shoot tissue grows tremendously while the root tissue is actually degraded during this same time (fig. 1). From this treadmilling, the dodder accomplishes something else important to ensure its survival: a net movement of the seedling in search of a host.

The dodder is a true minimalist in its approach. It has shed the traditional trappings of a plant: leaves, cotyledons, roots, and almost all chlorophyll. In this reduction, it has also set up a system for internal sustenance to support the growing seedling by effectively degrading and recycling its own seedling tissue to sustain the plant until a successful parasitic union is established. This only adds to the clever "bag of tricks" that the dodder has acquired to make it the most successful and widespread group of parasitic weeds.

Acknowledgments

These investigations were supported in part by an NRI grant to Kevin C. Vaughn. Dr. Timothy D. Sherman, Dr. T. Wayne Barger, and Dr. Andrew J. Bowling were supported by funds from the ARS Research Associate Program. Development and distribution of the antibodies designated CCRC were supported in part by NSF grants (DBI-0421683 and RCN-0090281). Thanks are extended to Brian Maxwell, Lynn Libous-Bailey, and Melyssa Bratton for their excellent technical assistance during the course of these experiments. Dr. John Hoffman assisted in some immunofluorescence experiments that are not shown in this article. Helpful comments from Rick Turley and Reiner Kloth are acknowledged. Mention of a trademark, proprietary product, or vendor does not constitute an endorsement by the USDA.

Literature Cited

Baskin TI, AS Betzner, R Hoggart, A Cork, RE Williamson 1992 Root morphology mutants in *Arabidopsis thaliana*. Aust J Plant Physiol 19: 427–437.

Baskin TI, JE Wilson, A Cork, RE Williamson 1994 Morphology and microtubule organization in *Arabidopsis* roots exposed to oryzalin or taxol. Plant Cell Physiol 35:935–942.

Bowling AJ, KC Vaughn 2008 Structural and immunocytochemical characterization of the adhesive tendril of Virginia creeper (*Parthenocissus quinquefolia* [L.] Planc.). Protoplasma 232:153–163.

Cesarone CF, C Bolognesi, L Santi 1979 Improved microfluorometric DNA determination in biological material using 33258 Hoechst. Anal Biochem 100:188–197.

Collings DA, CN Carter, JC Rink, AC Scott, SE Wyatt, N Strömgren-Allen 2000 Plant nuclei can contain extensive grooves and invaginations. Plant Cell 12:2425–2439.

Dawson JH, LJ Musselman, P Wolswinkel, I Dorr 1994 Biology and control of *Cuscuta*. Rev Weed Sci 6:265–317.

Evert RF 2006 Esau's plant anatomy: meristems, cells, and tissues of the plant body: their structure, function and development. 3rd ed. Wiley, Hoboken, NJ.

Gunawardena AHLAN, DME Pearce, MB Jackson, CR Hawes, DE Evans 2001*a* Characterisation of programmed cell death during aerenchyma formation induced by ethylene or hypoxia in roots of maize (*Zea mays* L.). Planta 212:205–214.

——— 2001*b* Rapid changes in cell wall polysaccharides are closely associated with early stages of aerenchyma formation, a spatially localized form of programmed cell death in roots of maize (*Zea mays* L.) promoted by ethylene. Plant Cell Environ 24:1369–1375.

Haccius B, W Troll 1961 Uber die sogenannte, Wurzelhaare an den Keimpflanzen von *Drosera*- und *Cuscuta*-Arten. Beitr Biol Pflanz 36:139–157.

Heide-Jorgenson HS 1987 Changes in cuticle structure during development and attachment of the upper haustorium of *Cuscuta* L., *Cassytha* L., and *Viscum* L. Pages 319–334 *in* HC Weber, W Forstreter, eds. Parasitic flowering plants. Proceedings of the 4th International Symposium on Parasitic Flowering Plants, Marburg, Germany.

Hoffman JC, KC Vaughn 1994 Mitotic disrupter herbicides act by a single mechanism but vary in efficacy. Protoplasma 179:16–25.

Kujit J 1969 The biology of parasitic flowering plants. University of California Press, Berkeley.

Lee KB 2007*a* Structure and development of the upper haustorium in the parasitic flowering plant *Cuscuta japonica* (Convulvaceae). Am J Bot 94:737–745.

——— 2007*b* Ultrastructure and development of seedlings of the parasitic weed *Cuscuta japonica*. J Plant Biol 50:213–219.

Lee KB, CD Lee 1989 The structure and development of the haustorium of *Cuscuta australis*. Can J Bot 67:2975–2982.

Lodhi MA, G-N Yee, NF Weeden, BI Reisch 1994 A simple and efficient method for DNA extraction from grapevine cultivars and *Vitis* species. Plant Mol Biol Rep 12:6–13.

Lyshede OB 1985 Morphological and anatomical features of *Cuscuta pedicellata* and *C. campestris*. Nord J Bot 5:65–77.

——— 1986 Fine-structural features of the tuberous radicular end of the seedling of *Cuscuta pedicellata*. Ber Dtsch Bot Ges 99:105–109.

——— 1989 Electron microscopy of the filiform seedling axis of *Cuscuta pedicellata*. Bot Gaz 150:230–238.

Malik CP, MB Singh 1979 Physiological and biochemical aspects of parasitism of *Cuscuta*: a review. Annu Rev Plant Sci 1979:319–326.

Meloche CG, JP Knox, KC Vaughn 2007 A cortical band of gelatinous fibers causes the coiling of redvine tendrils: a model based upon cytochemical and immunocytochemical studies. Planta 225:485–498.

Pena MJ, NC Carpita 2004 Loss of highly branched arabinans and de-branching of rhamnogalacturonan I accompany loss of firm texture and cell separation during prolonged storage of apple. Plant Physiol 135:1305–1313.

Rao PN, PV Rama Rao 1990 Not embryos but seedlings in seeds of *Cuscuta*. Indian J Bot 13:159–160.

Sabba RP, NA Durso, KC Vaughn 1999 Structural and immunocytochemical characterization of the walls of dichlobenil-habituated BY-2 tobacco cells. Int J Plant Sci 160:275–290.

Sambrook J, EF Fritsch, T Maniatis 1989 Molecular cloning: a laboratory manual. Cold Spring Harbor Press, Cold Spring, NY.

Schoenboek MA, GA Swanson, SJ Brommer 2007 ß-glucuronidase activity in seedlings of the parasitic angiosperm *Cuscuta pentagona*: developmental impact of the ß-glucoronidase inhibitor saccharic acid 1,4-lactone. Funct Plant Biol 34:811–821.

Sherman TD, WT Pettigrew, KC Vaughn 1999 Structural and immunological characterization of the *Cuscuta pentagona* chloroplast. Plant Cell Physiol 40:592–603.

Sommerville CR, WL Ogren 1982 Isolation of photorespiration mutants in *Arabidopsis thaliana*. Pages 129–136 *in* M Edelman, RB Hallick, NH Chua, eds. Methods in chloroplast molecular biology. Elsevier, New York.

Truscott FH 1966 Some aspects of morphogenesis in *Cuscuta gronovii*. Am J Bot 53:739–750.

Vaughn KC 2002*a* Attachment of the parasitic weed dodder to the host. Protoplasma 219:227–237.

——— 2002*b* Cellulose biosynthesis inhibitor herbicides. Pages 139–150 *in* P Böger, K Wakabayashi, K Hirai, eds. Herbicide classes in development: mode of action, targets, genetic engineering, chemistry. Springer, Heidelberg.

——— 2003 Dodder hyphae invade the host: a structural and immunocytochemical characterization. Protoplasma 220:189–200.

——— 2006 Conversion of the searching hyphae of dodder into xylic and phloic hyphae: a cytochemical and immunocytochemical investigation. Int J Plant Sci 167:1099–1114.

Vaughn KC, W Barger, D Cosgrove 2001 Dodders utilize expansin to attach to and to invade the host. Plant Biol 2001:17–18.

Vaughn KC, JC Hoffman, MG Hahn, LA Staehelin 1996 The herbicide dichlobenil disrupts cell plate formation: immunogold characterization. Protoplasma 194:117–132.

Vincken JP, HA Schols, RJFJ Oomen, MC McCann, P Ulvskov, AGJ Voragen, RGF Visser 2003 If homogalacturonan were a side chain of rhamnogalacturonan I: implications for cell wall architecture. Plant Physiol 132:1781–1789.